

Discrete Orthogonal Decomposition and Variational Fluid Flow Estimation

J. Yuan¹, P. Ruhnau¹, E. Mémin², and C. Schnörr¹

¹ Department of Mathematics and Computer Science
Computer Vision, Graphics, and Pattern Recognition Group
University of Mannheim, 68131 Mannheim, Germany
{yuanjing, ruhnau, schnoerr}@uni-mannheim.de
www.cvgpr.uni-mannheim.de

² IRISA Rennes
Campus Universitaire de Beaulieu
35042 Rennes Cedex, France
memin@irisa.fr
www.irisa.fr/vista

Abstract. The decomposition of motion vector fields into components of orthogonal subspaces is an important representation for both the analysis and the variational estimation of complex motions. Common finite differencing or finite element methods, however, do not preserve the basic identities of vector analysis. Therefore, we introduce in this paper the mimetic finite difference method for the estimation of fluid flows from image sequences. Using this discrete setting, we represent the motion components directly in terms of potential functions which are useful for motion pattern analysis. Additionally, we analyze well-posedness which has been lacking in previous work. Experimental results, including hard physical constraints like vanishing divergence of the flow, validate the theory.

1 Introduction

The estimation of highly non-rigid image flows is an important problem in various application areas of image analysis like remote sensing, medical imaging, and experimental fluid mechanics. Such flows, which cannot be represented by a single parametric model, are typically estimated by variational approaches. In contrast to standard approaches, however, higher-order regularization is necessary in order to accurately recover important flow structures like vortices, for example, and to incorporate physically plausible constraints, like vanishing divergence of the flow.

The basis for our paper is early work on second-order regularizers constraining the gradients of the flow components divergence and curl [1–3]. This regularization approach has been elaborated in a series of papers by Mémin and co-workers [4–6]. Moreover, the decomposition and representation of *continuous*

vector fields by velocity potentials and stream functions [7] has been adopted to derive piecewise parametric representations of relevant flow structures. Recently, the direct estimation of this representation has been studied in [8].

Contribution. From numerical fluid dynamics, it is well known that standard discretizations, like piecewise linear finite elements, are not appropriate. Imposing the constraint of vanishing divergence, for example, may result in a constant flow. Therefore, we introduce the mimetic finite difference method [9–11] to the field of image sequence analysis, which uses basic integral identities of vector analysis to derive discrete differential operators preserving these relationships *after* discretization. Based on this *exact* discrete representation, we study div-curl regularization, detect and remove a corresponding sensitivity of this regularizer to “boundary noise”, state precise conditions for well-posedness, and present a *provably convergent* iterative implementation for directly estimating velocity potentials and stream functions by iterative subspace correction. Most importantly, our approach makes the estimation of *accurate* solenoidal (non-divergent) flows feasible. The theory is validated by numerical experiments.

2 Vector-Field Representation

2.1 Discretization and Vector Spaces

We use the mimetic finite difference method for discretization [9, 10] in order to preserve basic relationships of continuous vector analysis. This discretization will be applied in section 2.2 to accurately represent and decompose vector fields.

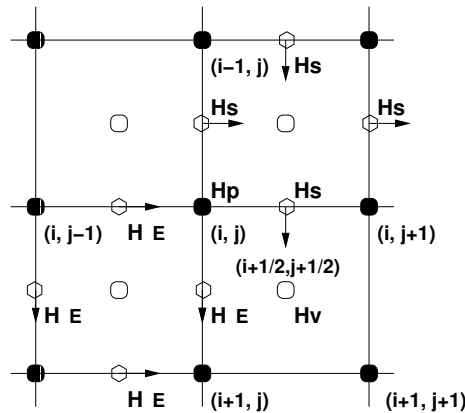


Fig. 1. Definition of finite-dimensional spaces of scalar fields and vector fields on a rectangular grid. Filled circles depict *nodes* or *vertices*, the other circles indicate *cells*. The positions of diamonds are referred to as *sides*.

Figure 1 illustrates the definitions of the following finite-dimensional vector spaces:

H_V : the space of *scalar fields* defined on cells,
 H_P : the space of *scalar fields* defined on vertices,
 H_E : the space of *vector fields* defined tangential to sides,
 H_S : the space of *vector fields* defined normal to sides.

Furthermore, we define the following *primal* discrete first-order differential operators:

$\mathbb{G} : H_P \rightarrow H_E$ the discrete gradient operator representing ∇ ,
 $\mathbb{G}^\perp : H_P \rightarrow H_S$ the discrete directional derivative along level curves representing ∇^\perp in the discrete case. This operator is specific to the 2D case considered here.
 $\mathbb{D}iv : H_S \rightarrow H_V$ the discrete divergence operator,
 $\mathbb{C}url : H_E \rightarrow H_V$ the discrete curl operator.

In order to construct the discrete second-order differential operators by combining first-order operators, *dual* discrete first-order differential operators

$\mathbb{G}^* : H_V \rightarrow H_S$, $\mathbb{G}^{\perp*} : H_V \rightarrow H_E$, $\mathbb{D}iv^* : H_E \rightarrow H_P$, $\mathbb{C}url^* : H_S \rightarrow H_P$

are defined so as to solve the incompatibilities of domains and ranges of the primal operators defined above [10]. For example, \mathbb{G} and $\mathbb{D}iv$ cannot be regarded as mutually adjoint operators like in the continuous case, whereas \mathbb{G} , $\mathbb{D}iv^*$ and \mathbb{G}^* , $\mathbb{D}iv$ do.

2.2 Orthogonal Decomposition

We represent vector fields directly in terms of their irrotational and solenoidal components. These components are defined by the first-order variations of velocity potentials ψ and stream functions ϕ , respectively [11]:

Theorem 1 (Vector Field Decomposition). *For any 2D vector field $u \in H_S$, the representation of u in terms of ψ , ϕ :*

$$u = \mathbb{G}^*\psi + \mathbb{G}^\perp\phi, \quad u_{\partial\Omega} = \partial_n\psi, \quad (1)$$

where $\phi_{\partial\Omega} = 0$, is unique up to a constant of ψ .

Here, Ω denotes the image section (grid), n the corresponding outer normal vector, and $f_{\partial\Omega}$ the boundary values of f . Let

$$u = v + w, \quad v = \mathbb{G}^*\psi, \quad w = \mathbb{G}^\perp\phi$$

according to (1). Since the operators defined in the previous section satisfy [11]:

$$\mathbb{D}iv \mathbb{G}^\perp \equiv 0, \quad \mathbb{C}url^* \mathbb{G}^* \equiv 0,$$

we have

$$\mathbb{D}iv w = 0, \quad \mathbb{C}url^* v = 0, \quad (2)$$

and:

$$\langle w, v \rangle_{H_S} = \langle \mathbb{G}^*\psi, \mathbb{G}^\perp\phi \rangle_{H_S} = \langle \mathbb{C}url^* \mathbb{G}^*\psi, \phi \rangle_{H_P} \equiv 0 \quad (3)$$

This shows:

Theorem 2 (Orthogonality). *The decomposition (1) is orthogonal, that is:*

$$\langle \mathbb{G}^* \psi, \mathbb{G}^\perp \phi \rangle_{H_S} = 0, \quad \forall u \in H_S \quad (4)$$

Let S_{ir} express the subspace of all vectors which can be written as $\mathbb{G}^* \psi$ and S_{sol} the subspace of vectors which can be represented as $\mathbb{G}^\perp \phi$. Then the previous theorem asserts that the direct sum holds:

$$H_S = S_{ir} \oplus S_{sol} \quad (5)$$

Representation (1) is motivated by analogous decompositions of continuous vector fields [7]. However, discretizing such vector fields with standard finite differences or finite elements yields *approximate* decompositions only, which may lead to numerical instabilities in applications. In contrast, theorem 1 provides an *exact* orthogonal decomposition of the *finite*-dimensional space of vector fields H_S . Furthermore, as detailed below, the decomposition allows to estimate ψ , ϕ directly, and in parallel, using variational optical flow approaches and subspace correction methods (cf. section 5.1).

Alternatively, we may first estimate u and then compute ψ and ϕ in a subsequent step by solving the Neumann and Dirichlet problems:

$$\Delta_D \psi = \mathbb{D}iv u, \quad \partial_n \psi = u_{\partial\Omega}, \quad (6)$$

$$\Delta_C \phi = \mathbb{C}url^* u, \quad \phi_{\partial\Omega} = 0, \quad (7)$$

where the discrete Laplacians are defined by:

$$\Delta_D := \mathbb{D}iv \mathbb{G}^*, \quad \Delta_C := \mathbb{C}url^* \mathbb{G}^\perp \quad (8)$$

and the additional constraint $\sum_{cells} \psi = 0$. In the remainder of this paper, however, we show that directly estimating ψ, ϕ from image sequence data is feasible.

3 Regularization and Optimization Problems

3.1 Representation of the Data Term and Linearization

We consider pixels as cells and define accordingly $I \in H_V$ for a given image.

We use the conventional data term for optical flow estimation, along with regularizers $L(u)$ to be specified below (section 3.2):

$$\min_{u \in H_S} F(u), \quad F(u) := \|I(x+u) - I(x)\|_{H_V}^2 + L(u) \quad (9)$$

Note that this data term could be made robust against outliers by using some robust estimators or the L^1 -norm [12]. In this paper, however, we focus on higher-order regularization in connection with the representation (1).

In order to alleviate the local minima problem, we apply the standard procedure of minimizing $F(u)$ using a sequence of linearizations of the data term:

$$F^l(u^l) := \|\mathbb{G}^* I_1^l \cdot u^l + \partial_t I^l\|_{H_V}^2 + L(u^l), \quad (10)$$

where $\{I_1^l, I_2^l\}_{l=0,1,\dots,m}$ denote linear scale-space representations of a given image pair, and $\partial_t I^l = I_1^l(x) - I_2^l(x + u^{l+1}(x))$.

3.2 Regularization

We wish to apply the following second-order regularizer (cf. the discussion of related work in section 1):

$$\int_{\Omega} \lambda_1 |\nabla \operatorname{div} u|^2 + \lambda_2 |\nabla \operatorname{curl} u|^2 dx \quad (11)$$

where λ_1 and λ_2 are two positive constants. This term measures the variation of the basic flow components divergence and curl, but *does not penalize* the components itself. However, both standard finite differences or finite elements discretization lead to finite-dimensional representations which do not satisfy (1), (4). As a result, penalizing one component may affect the other component too. Therefore, we adopt the framework sketched in section 2.1 which leads to the following discretization of (11):

$$L(u) := L_{div}(u) + L_{curl}(u) := \lambda_1 \|\mathbb{G}^* \mathbb{D}iv u\|_{H_S}^2 + \lambda_2 \|\mathbb{G} \mathbb{C}url^* u\|_{H_E}^2, \quad (12)$$

3.3 Estimation of Non-rigid Flows

Based on (12), we consider the functional:

$$\min_{u \in H_S} F(u) := \|I(x+u) - I(x)\|_{H_V}^2 + L_{div}(u) + L_{curl}(u) \quad (13)$$

Inserting the decomposition (1), we obtain the minimization problem:

$$\begin{aligned} \min_{\psi, \phi} F(\psi, \phi) &= \|I(x + \mathbb{G}^* \psi + \mathbb{G}^\perp \phi) - I(x)\|_{H_V}^2 \\ &+ \lambda_1 \|\mathbb{G}^* \Delta_D \psi\|_{H_S}^2 + \lambda_2 \|\mathbb{G} \Delta_C \phi\|_{H_E}^2 \end{aligned} \quad (14)$$

subject to the linear constraints:

$$\sum_{cells} \psi = 0, \quad \phi_{\partial\Omega} = 0 \quad (15)$$

Note that the first constraint fixes the free constant mentioned in theorem 1. Furthermore, the arguments of (14) are elements of orthogonal subspaces (5), and thus may be determined in parallel by subspace correction methods.

3.4 Estimation of Solenoidal Flows

An important special case, particularly in applications of experimental fluid dynamics, concerns the estimation of solenoidal (divergence-free) flows. In this case the decomposition (1) reduces to:

$$u = \mathbb{G}^* \psi_l + \mathbb{G}^\perp \phi := u_l + \mathbb{G}^\perp \phi \quad (16)$$

where the *laminar flow* u_l can be computed through the full flow u by solving:

$$\Delta_D \psi_l = 0, \quad \partial_n \psi_l = u_{\partial\Omega} \quad (17)$$

and $u_l = \mathbb{G}^* \psi_l$. Since $\mathbb{C}url^* \mathbb{G}^* \equiv 0$, the laminar flow u_l is both divergence and curl free. In order for (17) to be solvable, we require the compatible condition $\int_{\partial\Omega} u_{\partial\Omega} dl = 0$ (cf., e.g., [13]).

Let $S_{div0} = \{u \in H_S \mid \mathbb{D}iv u = 0\}$ be the linear space of vector fields with vanishing divergence. Then the following direct sum holds:

$$S_{div0} = S_{lam} \oplus S_{sol} \quad (18)$$

with laminar and solenoidal flows as basic components.

In order to estimate solenoidal flows, we consider instead of (13) the functional:

$$\min_{u \in S_{div0}} F_{sol}(u) := \|I(x+u) - I(x)\|_{H_V}^2 + L_{curl}(u) \quad (19)$$

which is well-defined by (18). Inserting the decomposition (16), we obtain the minimization problem:

$$\min_{\psi_l, \phi} F_{sol}(\psi_l, \phi) = \|I(x + \mathbb{G}^* \psi_l + \mathbb{G}^\perp \phi) - I(x)\|_{H_V}^2 + \lambda \|\mathbb{G} \Delta_C \phi\|_{H_E}^2 \quad (20)$$

subject to the constraints:

$$\Delta_D \psi_l = 0, \quad \sum_{cells} \psi_l = 0, \quad \phi_{\partial\Omega} = 0 \quad (21)$$

Note that the arguments of (20) are elements of orthogonal subspaces (18), and thus may be determined in parallel by subspace correction methods.

4 Well-Posedness and Stability

4.1 Well-Posedness

We state the conditions under which the functionals (13) and (19) with *linearized* data terms (cf. (10)) are strictly convex. To this end, we consider the spaces:

$$\begin{aligned} S_d &= \{u \in H_S \mid \mathbb{D}iv u = C, \mathbb{C}url^* u = 0, C \in \mathbb{R} \text{ arbitrary}\} \\ S_c &= \{u \in H_S \mid \mathbb{D}iv u = 0, \mathbb{C}url^* u = C, C \in \mathbb{R} \text{ arbitrary}\} \\ S_{dc} &= \{u \in H_S \mid u = u_1 + u_2, u_1 \in S_d, u_2 \in S_c\} \\ S_g &= \{u \in H_S \mid \mathbb{G}^* I_1 \cdot u = 0\} \end{aligned}$$

As we work with finite-dimensional vector fields, the following two assertions are obvious: problem

$$\min_{u \in H_S} F(u) := \|\mathbb{G}^* I_1 \cdot u + \partial_t I\|_{H_V}^2 + \lambda_1 \|\mathbb{G}^* \mathbb{D}iv u\|_{H_S}^2 + \lambda_2 \|\mathbb{G} \mathbb{C}url^* u\|_{H_E}^2 \quad (22)$$

is strictly convex iff the subspaces S_g and S_{dc} trivially intersect, that is there is no vector $0 \neq u \in S_{dc}$ which is perpendicular to $\mathbb{G}^* I_1$. Similarly, problem

$$\min_{u \in S_{div0}} F_{sol}(u) := \|\mathbb{G}^* I_1 \cdot u + \partial_t I\|_{H_V}^2 + \lambda \|\mathbb{G} \mathbb{C}url^* u\|_{H_E}^2 \quad (23)$$

is strictly convex iff S_g and S_c trivially intersect.

4.2 Stability

It is well-known that existence of a unique solution, as established in the previous section, does not say much about *numerical* stability. Indeed, inspection of the second-order regularizer (11) reveals a particular sensitivity of u with respect to the image data, and suggests using a corresponding regularizer.

To motivate this additional term, we consider the following representation of vector fields u in terms of functions ρ, ω and boundary data v :

$$\operatorname{div} u = \rho, \quad \operatorname{curl} u = \omega, \quad u_{\partial\Omega} = v$$

Provided the compatibility condition:

$$\int_{\Omega} \rho \, dx = \int_{\partial\Omega} v \, dl \tag{24}$$

holds, u is uniquely defined, both in the continuous case [13] and in the discrete case, using the discretization of section 2.1.

It is clear that the regularizer (11) only constrains ρ and ω , but *not* v which is weakly constrained only through the data terms of the functionals considered above. Therefore, in practice, it turned out to be useful to reduce this sensitivity of u by including a regularizer which weakly constrains the boundary values:

$$\int_{\partial\Omega} (\partial_n u)^2 \, dl. \tag{25}$$

By virtue of the orthogonal decomposition, this constraint can be expressed in terms of ψ .

5 Experiments and Discussion

5.1 Implementation Details

Minimization of the functionals (14) and (20), respectively, with linearized data terms (see (10)) can be done by alternating partial minimizations with respect to ψ , ϕ and subsequent subspace corrections. The proof of convergence and further details are given in [14, 15]. In the case of solenoidal flows, the first linear constraint in (21) is incorporated by using the Augmented Lagrangian Method [16]. The remaining two constraints can be taken into account by directly modifying the two linear systems involved.

5.2 Experiment Results

Error measures. In practice, evaluating non-rigid flows by computing the average angular and norm error, respectively, induced by the inner product of the

space $(L^2(\Omega))^2 = L^2(\Omega) \times L^2(\Omega)$ [17] appeared to us too insensitive to the important flow structures. Therefore, we suggest error measures that also take into account divergence and curl of flow structures:

$$e_{norm} = \frac{\langle w, w \rangle_{DC}}{N}; \quad e_{ang.} = \arccos \frac{\langle u, v \rangle_{DC} + 1}{\sqrt{\langle u, u \rangle_{DC} + 1} \sqrt{\langle v, v \rangle_{DC} + 1}}. \quad (26)$$

where we adopt the average angular and norm error measures but use the inner products of the space $H(\text{div}; \Omega) \cap H(\text{curl}; \Omega)$ (see, e.g., [7]):

$$\langle u, v \rangle_{DC} = \langle u, v \rangle_{H_S} + \langle \text{Div } u, \text{Div } v \rangle_{H_V} + \langle \text{Curl }^* u, \text{Curl }^* v \rangle_{H_P}. \quad (27)$$

Ground truth experiments. Figure 2 shows a real image which was warped by the flow shown on the right. The corresponding errors for the approach (20) $e_{norm} = 6.1 * 10^{-3}$, $e_{ang.} = 6.51^\circ$ are smaller than the approach with Horn-Schunck regularization, for which $e_{norm} = 2.95 * 10^{-2}$, $e_{ang.} = 13.52^\circ$. Note, that these error measures include flow derivatives as opposed to common measures used in the literature.

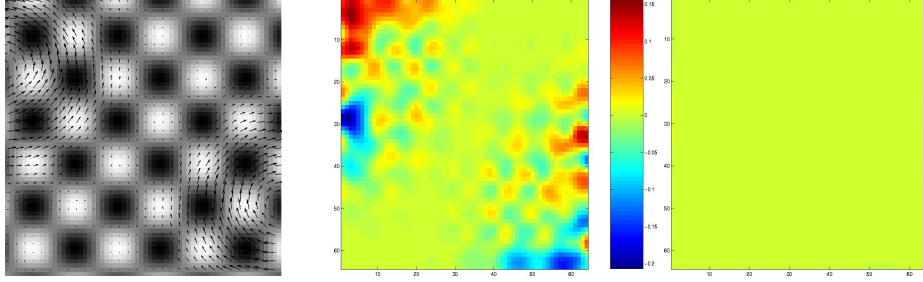


Fig. 2. **Left:** Synthetic image and solenoidal velocity field. **Middle:** Divergence error using Horn-Schunck regularization. **Right:** Divergence error using our approach.

Estimating solenoidal flows. Figure 3 shows the result of estimating the solenoidal flow for a real image sequence. The comparison with first-order regularization (Horn-Schunck approach) in Figure 4 clearly reveals the superiority of our approach regarding the reconstruction of vortex structures. Furthermore, the (in this case) physically plausible constraint of vanishing divergence is satisfied quite accurately.

Estimating general non-rigid flows. Figures 5 and 6 show general non-rigid flow estimated for two different real image sequences. As in the solenoidal case, the potential functions provide a useful representation of qualitative properties of the flow.

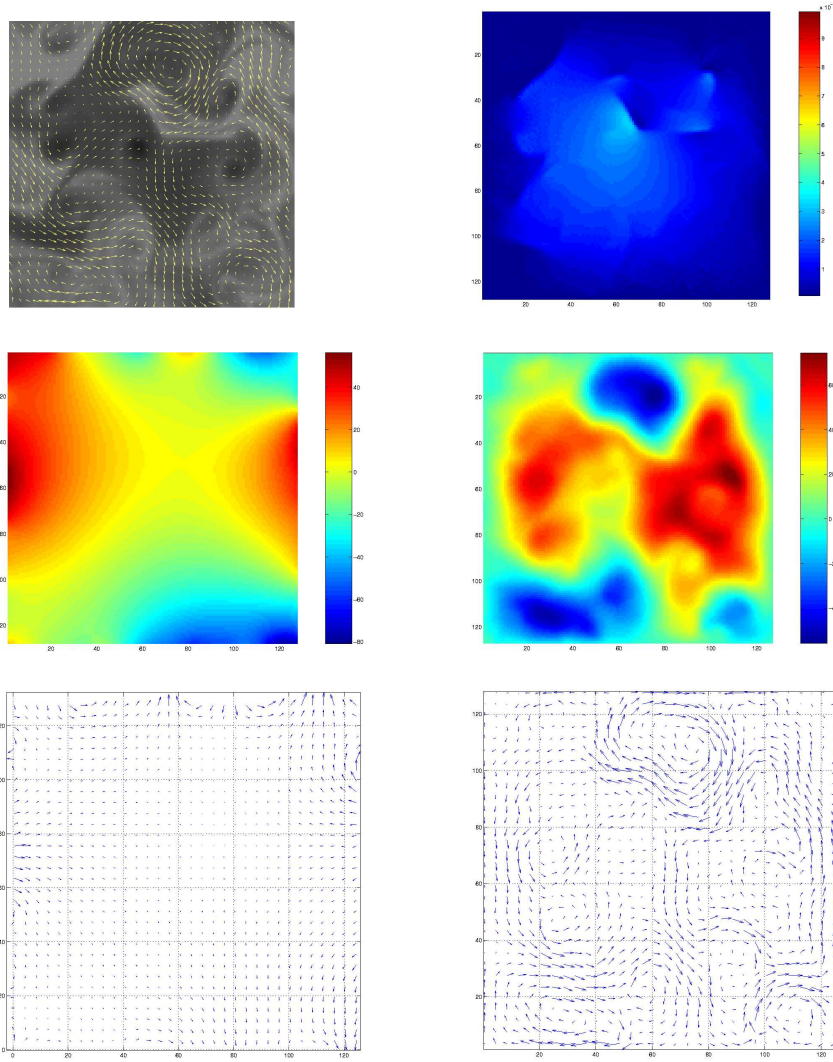


Fig. 3. **Top Left** The first image I_1 with the restored solenoidal flow. **Top Right** The divergence field of the flow which is less than $3 * 10^{-12}$. **Middle Left** The potential field $\psi_l(\Omega)$ related to the laminar flow. **Middle Right** The potential field $\phi(\Omega)$. **Bottom Left** The first component of flow: the laminar flow u_{lam} . **Bottom Right** The second component of flow related to potential $\phi(\Omega)$. The comparison with standard regularization is depicted in Figure 4.

6 Conclusion and Future Works

We presented a high-quality discrete representation of flow estimation schemes for non-rigid flows. Our further work will focus on the extension to 3D image sequences.

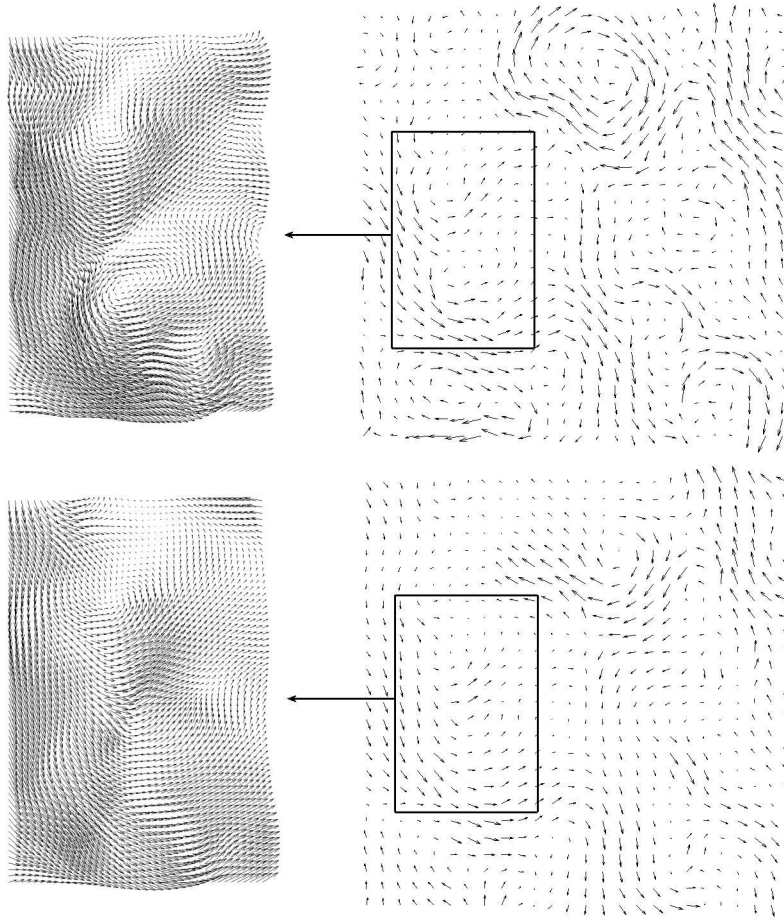


Fig. 4. Top The restored solenoidal flow $u(\Omega)$. **Bottom** The restored flow $u_{hs}(\Omega)$ using the Horn-Schunck regularization. This results clearly show that vortex structures are better recovered by our approach. Furthermore, the magnitude of the divergence is below 10^{-11} throughout the image plane.

References

1. L. Amodei and M. N. Benbourhim. A vector spline approximation. *J. Approx. Theory*, 67(1):51–79, 1991.
2. D. Suter. Motion estimation and vector splines. In *Proceedings of the Conference on Computer Vision and Pattern Recognition*, pages 939–942, Los Alamitos, CA, USA, June 1994. IEEE Computer Society Press.
3. S. Gupta and J. Prince. Stochastic models for div-curl optical flow methods. *Signal Proc. Letters*, 3(2):32–34, 1996.
4. T. Corpetti, É. Mémin, and P. Pérez. Dense motion analysis in fluid imagery. *Lecture Notes in Computer Science*, 2350:676–691, 2002.

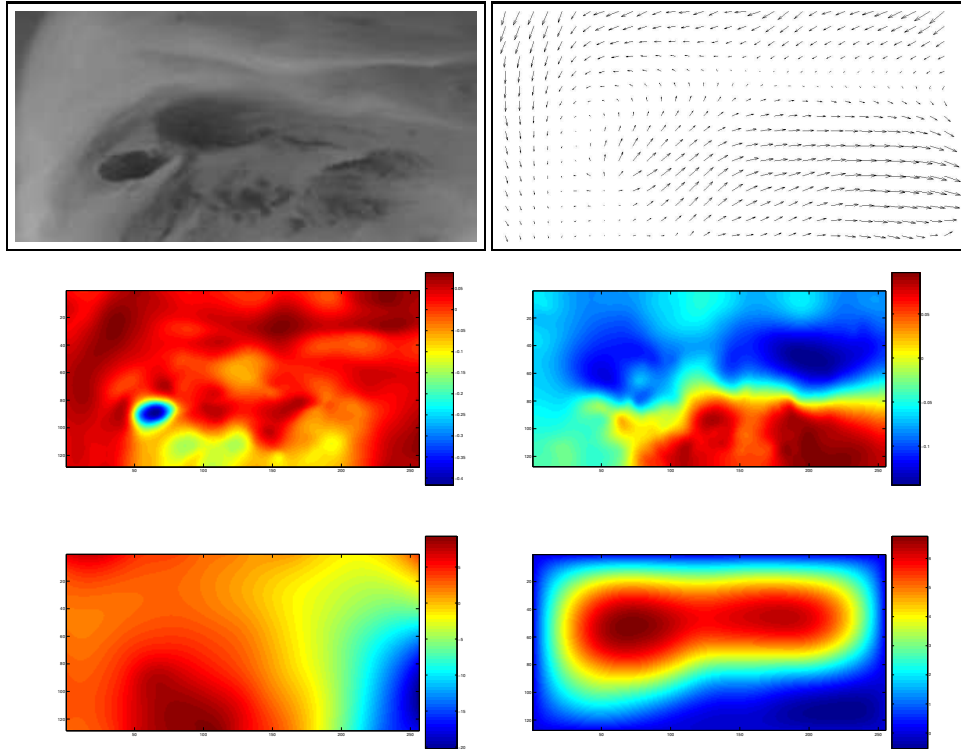


Fig. 5. **Top Left** Image I with the restored flow field u . **Middle Left** The divergence field of u . **Middle Right** The curl field of u . **Bottom Left** The potential field $\psi(\Omega)$. **Bottom Right** The potential field $\phi(\Omega)$. The divergence field, for example, which clearly detects a “source” (blue blob), illustrates the quality and usefulness of the results.

5. T. Corpetti, E. Mémin, and P. Pérez. Dense estimation of fluid flows. *IEEE Trans. Pattern Anal. Machine Intell.*, 24(3):365–380, 2002.
6. T. Corpetti, E. Mémin, and P. Pérez. Extraction of singular points from dense motion fields: an analytic approach. *J. of Math. Imag. Vision*, 19(3):175–198, 2003.
7. V. Girault and P.-A. Raviart. *Finite Element Methods for Navier-Stokes Equations*. Springer, 1986.
8. T. Kohlberger, E. Mémin, and C. Schnörr. Variational dense motion estimation using the helmholtz decomposition. In L.D. Griffin and M. Lillholm, editors, *Scale Space Methods in Computer Vision*, volume 2695 of *LNCS*, pages 432–448. Springer, 2003.
9. James M. Hyman and Mikhail J. Shashkov. Natural discretizations for the divergence, gradient, and curl on logically rectangular grids. *Comput. Math. Appl.*, 33(4):81–104, 1997.
10. James M. Hyman and Mikhail J. Shashkov. Adjoint operators for the natural discretizations of the divergence, gradient and curl on logically rectangular grids. *Appl. Numer. Math.*, 25(4):413–442, 1997.

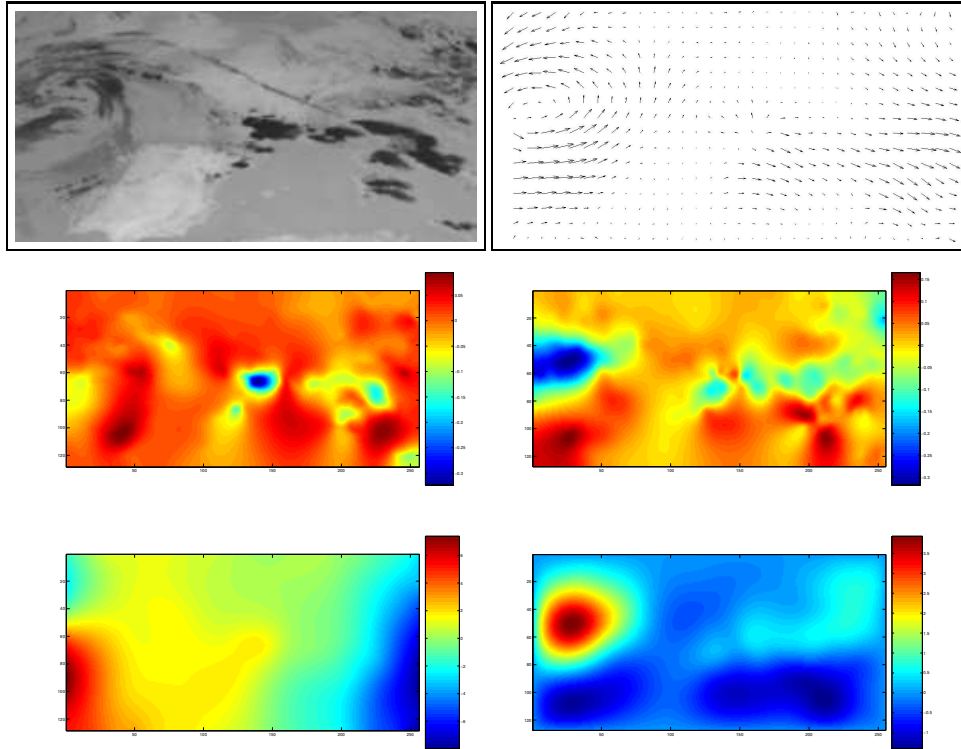


Fig. 6. **Top** Image I with the restored flow field u . **Middle Left** The divergence field of u . **Middle Right** The curl field of u . **Bottom Left** The potential field $\psi(\Omega)$. **Bottom Right** The potential field $\phi(\Omega)$. As in the previous figure, the potential functions provide a useful representation of qualitative properties of the flow.

11. James M. Hyman and Mikhail J. Shashkov. The orthogonal decomposition theorems for mimetic finite difference methods. *SIAM J. Numer. Anal.*, 36(3):788–818 (electronic), 1999.
12. M. J. Black and P. Anandan. The robust estimation of multiple motions: Parametric and piecewise-smooth flow fields. *Computer Vision and Image Understanding*, 63(1):75–104, 1996.
13. Lawrence C. Evans. *Partial differential equations*, volume 19 of *Graduate Studies in Mathematics*. American Mathematical Society, Providence, RI, 1998.
14. J. Xu. Iterative methods by space decomposition and subspace correction: A unifying approach. *SIAM Review*, 34:581–613, 1992.
15. Xue-Cheng Tai and Jinchao Xu. Global and uniform convergence of subspace correction methods for some convex optimization problems. *Math. Comp.*, 71(237):105–124 (electronic), 2002.
16. D. P. Bertsekas. *Nonlinear Programming*. Athena Scientific, Belmont, MA, 1995. 2nd edition 1999.
17. J. L. Barron, David J. Fleet, and S. S. Beauchemin. Performance of optical flow techniques. *International Journal of Computer Vision*, 12(1):43–77, 1994.